Tilted precession and wobbling in triaxial nuclei

E. A. Lawrie [1,2,*] O. Shirinda [1,†] and C. M. Petrache [3,‡]

[1] *iThemba LABS, National Research Foundation, PO Box 722, Somerset West 7129, South Africa*

[2] *Department of Physics, University of the Western Cape, Private Bag X17, 7535 Bellville, South Africa*

[3] *Centre de Sciences Nucléaires et de Sciences de la Matière, CNRS/IN2P3, Université Paris-Saclay, Bâtiment 104-108, 91405 Orsay, France*

(Received 16 October 2019; accepted 24 February 2020; published 16 March 2020)

The rotation of a triaxial nucleus can be represented (in a semiclassical description) as a precession of the total angular momentum around a certain axis and at a given tilt, producing tilted precession (TiP) bands. Such bands are described by rotational models and can in principle be approximated with wobbling. We studied for which TiP bands such an approximation is justified. It was found that TiP bands become approximately similar to wobbling bands at high spins for both zero-seniority bands in even-even nuclei, and one-quasiparticle bands with longitudinal coupling of the angular momenta in odd-mass nuclei. Contrary to that, the precession for transverse coupling of the angular momenta in one-quasiparticle configurations giving rise to TiP bands cannot be approximated with wobbling either at low or at high spins. This suggests that the interpretation of a band in terms of transverse wobbling cannot be justified only by particle-rotor-type model, as this model implies a different, TiP, nature. Contrary to TiP bands, the transverse wobbling bands exhibit quantized excitation energies and transition probabilities which is typical for bands involving phonon excitations.

DOI: 10.1103/PhysRevC.101.034306

I. INTRODUCTION

When collective degrees of freedom are dominant the complex many-body nuclear system can show surprisingly simple excitation spectra. For instance a rotating even-even nucleus shows a regular sequence of excited states with excitation energy of $E \propto I(I+1)$, called a rotational band. If the nuclear shape is triaxial the rotational spectrum becomes more complex: in addition to the ground-state rotational band, a series of excited rotational bands, often called γ bands, are generated. These excited bands result from the more complicated three-dimensional (3D) rotation of the nucleus, proceeding simultaneously around the three nuclear axes.

In the last few years a very interesting new phenomenon, called transverse wobbling, was introduced [1]. It occurs under the constraining assumption that the angular momentum of a valence nucleon is frozen along the nuclear axis with intermediate moment of inertia, and is associated with the coupling of rotational and vibrational degrees of freedom. It was derived through an approximation of the rotating Hamiltonian, where the 3D rotation was replaced by a simple 1D rotation, coupled to an excitation of wobbling phonons.

Recently a number of rotational bands have been interpreted as generated by transverse wobbling. For instance two rotational bands in ^{135}Pr, built on a $\pi h_{11/2}$ configuration, were suggested as one-phonon and two-phonon transverse wobbling excitations, respectively, with respect to the yrast $\pi h_{11/2}$ band [1–3]. One band in ^{105}Pd, built on a $\nu h_{11/2}$ configuration, was also interpreted as having a one-phonon transverse wobbling nature [4]. Furthermore, the triaxial superdeformed bands (TSD) in the odd-mass Lu isotopes, built on $\pi i_{13/2}$ configurations [5–15], were recently reinterpreted as also caused by transverse wobbling [1].

However, the bands discussed in these recent works have been compared not with the transverse wobbling equations as given in Ref. [1], but with a quasiparticle-plus-triaxial-rotor (QTR) model. As this rotational model describes 3D rotation and not wobbling, it is not obvious whether it is an adequate tool to justify transverse wobbling.

The transverse wobbling approximation in Ref. [1] was derived in the same way as Bohr and Mottelson derived the wobbling approximation for a simple wobbler (a zero-quasiparticle configuration in even-even nuclei) [16]. In this work the wobbling approximation in even-even nuclei is first presented as in previous textbooks like, e.g., Ref. [16], also evaluating the values of the approximation condition function in order to judge on the adequacy of the wobbling approximation. Then the wobbling in odd-mass nuclei assuming frozen angular momentum of the valence particle is investigated, with the aim to establish to what extent and under which conditions the particle-rotor Hamiltonian can be approximated with wobbling phonon excitations. We found that the QTR model and the transverse wobbling approximation describe rotational bands with different properties. In addition, the present analysis highlights the characteristic features of the transverse wobbling bands, and shows how to distinguish transverse wobbling from 3D rotation.

*elena@tlabs.ac.za

†obed@tlabs.ac.za

‡petrache@csnsm.in2p3.fr

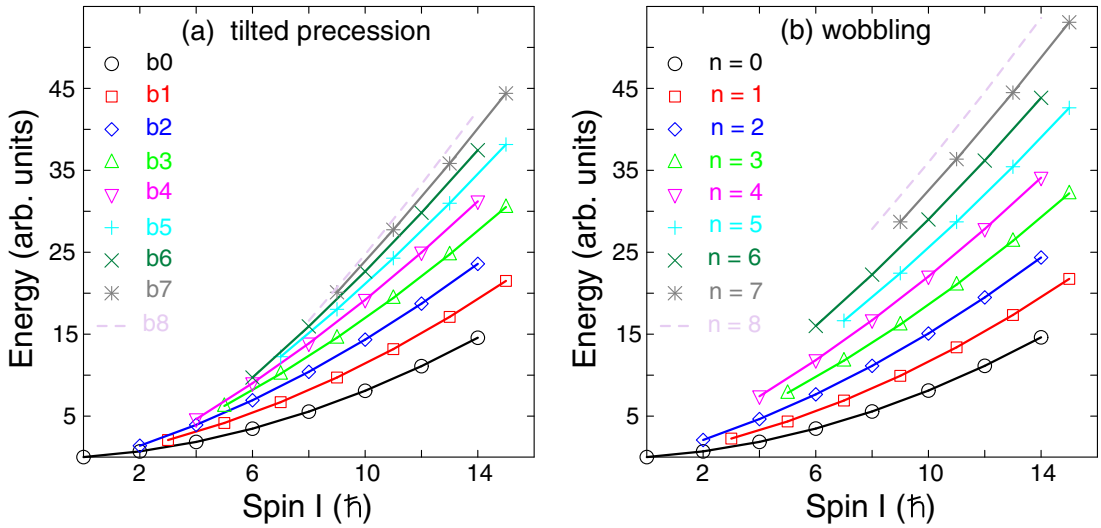

FIG. 1. Excitation energy vs spin in even-even nuclei with rotational parameters of $A_1 = 1$, $A_2 = 4$, and $A_3 = 4$, for (a) 3D rotation [Eq. (2)], and (b) wobbling [Eq. (9)].

II. TILTED PRECESSION AND WOBBLING IN EVEN-EVEN NUCLEI

A deformed triaxial nucleus rotates around each of its three axes. Therefore

$$H = A_1 R_1^2 + A_2 R_2^2 + A_3 R_3^2, \tag{1}$$

where the rotational parameters A_1, A_2, and A_3 depend on the corresponding moments of inertia (MoI), for instance $A_1 = \hbar^2/2\Im_1$, and the projections of the rotational angular momentum along the three axes are R_1, R_2, and R_3, respectively. For a rotating even-even nucleus (with no valence nucleons outside the core) the projections of the rotational angular momenta are equal to those of the total angular momentum, thus

$$H = A_1 I_1^2 + A_2 I_2^2 + A_3 I_3^2. \tag{2}$$

The solutions of this Hamiltonian describe a series of rotational bands, including the ground-state (gs) band and what is often called the γ bands; see, for example, Fig. 1(a), which shows the 3D rotational Hamiltonian, solved with an irrotational flow type of the MoI, (where $\Im_k = \Im_0 \frac{4}{3}\sin^2(\gamma - \frac{2}{3}\pi k)$, $k = 1, 2, 3$), and triaxiality parameter $\gamma = 30^\circ$. The choice of an irrotational flow MoI is supported by a previous work showing that the empirical MoI follows closely the trend of the irrotational flow MoI as a function of the γ deformation [17]. For such MoI the intermediate axis (1 axis) is the axis with largest MoI, while for $\gamma = 30^\circ$ the MoI along the short and long axes are identical.

To understand the nature of the rotational bands we discuss in more detail the example shown in Fig. 1(a). Due to the symmetry of the Hamiltonian (for $\gamma = 30^\circ$, $\Im_2 = \Im_3$) the projection of the rotational angular momentum R_1 along the intermediate axis is a good quantum number, i, and an even integer. The Hamiltonian is [18]

$$\begin{aligned} H &= \frac{3\hbar^2}{8\Im_0}\left\{R_1^2 + 4\left(R_2^2 + R_3^2\right)\right\} \\ &= \frac{3\hbar^2}{8\Im_0}\left\{R_1^2 + 4\left[I(I+1) - R_1^2\right]\right\}. \end{aligned} \tag{3}$$

Therefore the excitation energy of the rotational state with angular momentum I and projection i on the 1 axis is

$$E(I, i) = \frac{3\hbar^2}{8\Im_0}\{4I(I+1) - 3i^2\}. \tag{4}$$

The ground-state band, $b0$ in Fig. 1, corresponds to $E(I, i = I)$, that is, to rotation with maximum angular momentum projection on the intermediate axis. Contrary to that, the excited γ bands are generated when $R_1 < I$, that is when the rotational angular momentum is tilted away from the intermediate axis. For instance the odd and the even signatures of the first γ-band correspond to $i = I - 1$ and $i = I - 2$, respectively. These are the $b1$ and $b2$ bands in Fig. 1(a). Similarly the odd- and even-spin sequences of the next γ band, bands $b3$ and $b4$ in Fig. 1(a), correspond to a further tilt away of the rotational angular momentum, with projections on the intermediate axis of $i = I - 3$ and $i = I - 4$, respectively.

Note that the nature of the γ bands within the rotational model is different from the $K = 2$, $K = 4$, etc., γ bands produced by the Bohr Hamiltonian. In the latter case the $K = 2$ γ band, for instance, is produced by a zero-phonon vibration coupled with $K = 2$ rotation, where K is the projection of the total angular momentum on the symmetry axis of an axially symmetric nucleus. Contrary to that, the γ bands produced by 3D rotation exist for triaxial nuclei only, and cannot be associated with a sharp quantum number K. To highlight the difference between these two types of γ bands, the 3D rotational bands in triaxial nuclei are called, in the following, tilted precession (TiP) bands. More details on the nature of these bands are given below.

Three-dimensional rotation can be visualized in a semiclassical description (as suggested in Ref. [1]), as a precession of the total angular momentum vector around the intermediate axis. For instance, the classical rotational angular momentum $\vec{R}$ (in this case equal to the total angular momentum $\vec{I}$) is confined by the conservation of the momentum and energy

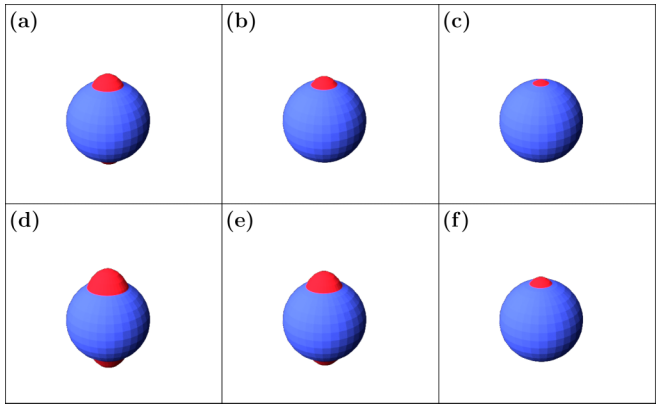

FIG. 2. Schematic illustration of the trajectory of the rotational angular momentum. It moves along the intersection of the angular momentum sphere (in blue) and the energy ellipsoid (in red). Panels (a)–(c) correspond to a band (e.g., $b1$) and illustrate the precession as the spin I increases. Panels (d)–(f) represent an excited band (e.g., $b2$) as a function of spin. The rotational parameters are $A_1 = 1, A_2 = 4$, and $A_3 = 4$.

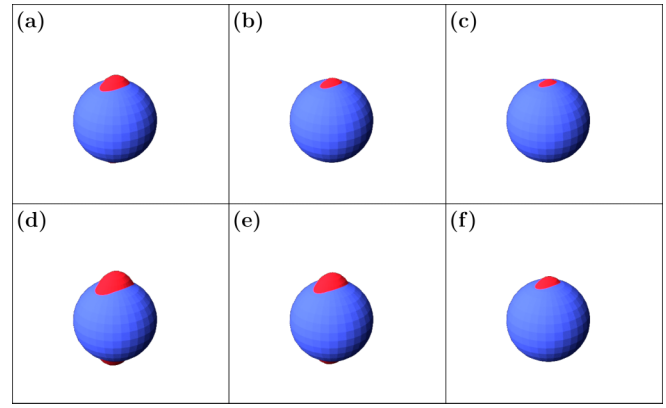

FIG. 3. As in Fig. 2, but for rotational parameters of $A_1 = 1$, $A_2 = 3$, and $A_3 = 6$.

laws to the intersection of the total angular momentum sphere:

$$I^2 = I_1^2 + I_2^2 + I_3^2, \tag{5}$$

and the energy ellipsoid:

$$E = A_1 I_1^2 + A_2 I_2^2 + A_3 I_3^2. \tag{6}$$

For the example shown in Fig. 1 the energy ellipsoid is a spheroid ($A_2 = A_3$) and intersects the angular momentum sphere as shown in Fig. 2(a). The intersection curve is a circle. Therefore the 3D rotation in this case looks like a precession of the total angular momentum around the intermediate axis, producing TiP bands.

To generate rotational states at higher spins the radius of the angular momentum sphere should increase. The corresponding energy ellipsoid will also be larger, while the intersection curve will again be a circle; see Figs. 2(b) and 2(c). One can estimate the tilt angle for the yrast rotational band as $\cos\theta = I/\sqrt{I(I+1)}$, therefore θ decreases at higher spins, as illustrated in Figs. 2(b) and 2(c).

If the three rotational parameters have nonequal values, for instance $A_1 = 1, A_2 = 3$, and $A_3 = 6$, the energy ellipsoid intersects with the angular momentum sphere as shown in Fig. 3(a). The angular momentum vector in this case is confined on an elliptic curve lying on the surface of the sphere. For higher-spin states the intersection curve remains similar, with a decreasing tilt angle θ, as shown in Figs. 3(b) and 3(c), corresponding to TiP bands.

To generate excited rotational bands one has to increase the rotational energy while keeping the magnitude of the angular momentum the same. The larger-size energy ellipsoid will intersect with the same-size angular momentum sphere in a similar way as in Figs. 2(a) and 3(a), but at a larger precession angle θ; see panels (d)–(f) of Figs. 2 and 3, respectively. Therefore the excited TiP bands correspond to a larger tilt of the rotational angular momentum.

This description is in agreement with Eq. (4) which suggests that the excited TiP bands (with $i < I$) correspond to a tilting of the rotational angular momentum vector away from the intermediate axis, since for the same I the projection on the intermediate axis i is smaller. This is not surprising, as it is clear that the only way to produce an excited rotational band (without introducing other degrees of freedom) is by tilting the rotational angular momentum away from the axis with largest MoI.

There is an alternative way to visualize the orientation of the total angular momentum, by plotting the probability distribution of the total angular momentum angles (θ, ϕ) calculated with the QTR model; see [19,20]. In these works calculations were carried out for two-quasiparticle chiral configurations, and showed specific peaks of the probability distributions at particular (θ, ϕ) values. These peaks suggest that the total angular momentum does not precess around a major nuclear axis, because such a precession would show as a ridge. For instance a precession around the 3 axis (long axis), would correspond to a vertical ridge at a specific θ, covering all angles of $\phi = (0^\circ, 180^\circ)$.

One could question whether the TiP bands produced by 3D rotation might not have a similar nature as what is known as wobbling bands. Indeed, wobbling bands are generated by tilting the rotational angular momentum away from the axis of rotation. However, contrary to TiP, the wobbling motion is commonly defined as a coupling of a 1D rotation with an excitation of wobbling phonons. Can these two different types of motion be, in some cases, similar?

The approximation of 3D rotation in even-even triaxial nuclei with wobbling was first studied by Bohr and Mottelson [16]. They found that it was possible to make such an approximation:

$$H = A_1 I_1^2 + A_2 I_2^2 + A_3 I_3^2 \approx A_1 I^2 + \tfrac{1}{2}\alpha(c^+ c + c c^+) + \tfrac{1}{2}\beta(c^+ c^+ + cc), \tag{7}$$

where the wobbling phonons were described by the creation (c^+) and annihilation (c) operators, and the coefficients α and β (assuming $A_1 \leqslant A_2 \leqslant A_3$) were

$$\alpha = (A_2 + A_3 - 2A_1)I, \quad \beta = (A_2 - A_3)I. \tag{8}$$

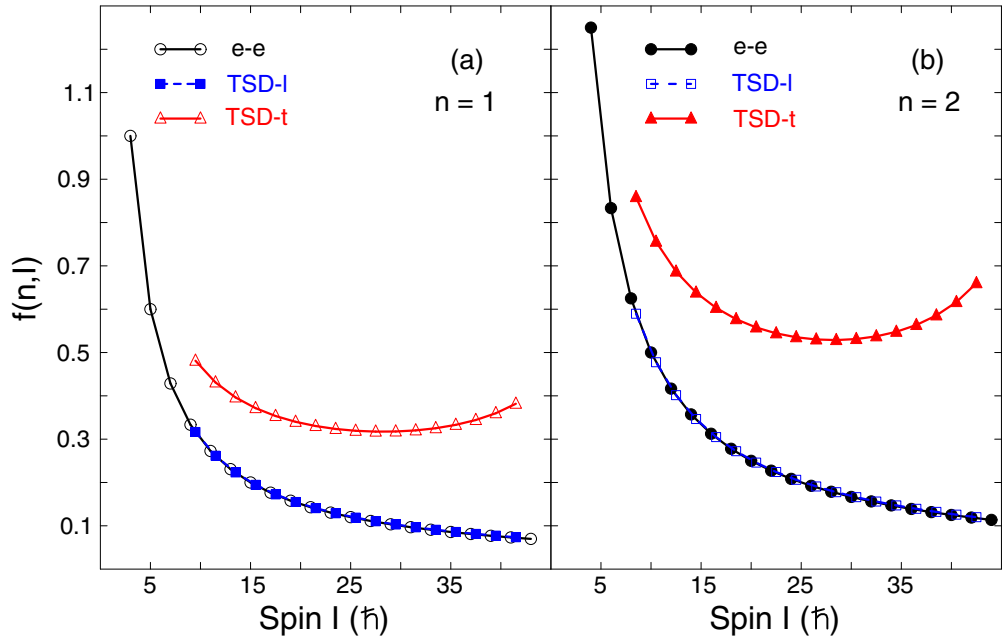

FIG. 4. Approximation condition function $f(n, I)$ for (a) the $n = 1$ and (b) $n = 2$ wobbling phonon bands, and for even-even (e-e) nuclei and for the TSD bands in the Lu isotopes assuming longitudinal (TSD-l) and transverse (TSD-t) coupling of the angular momenta, respectively. Rotational parameters of $A_1 = 1$, $A_2 = 4$, and $A_3 = 4$ are used for even-even nuclei. The rotational parameters for TSD-t and TSD-l are listed in Table I as (vii) and (viii), respectively.

The wobbling approximation produces a set of rotational bands, called wobbling bands. The excitation energy of the band with n excited phonons is

$$E(n, I) = A_1 I(I + 1) + \hbar\omega\left(n + \tfrac{1}{2}\right), \tag{9}$$

where the wobbling frequency is

$$\hbar\omega = \sqrt{(\alpha^2 - \beta^2)} = 2I\sqrt{(A_2 - A_1)(A_3 - A_1)}. \tag{10}$$

Each wobbling band corresponds to the excitation of an additional wobbling phonon. Each phonon causes an additional tilt of the rotational angular momentum away from the 1 axis. There is a quantization rule for the energies and transition probabilities of the wobbling bands, for instance: (i) the energy of the band depends linearly on n, see Eq. (9); (ii) the intraband $B(E2)$ transition probabilities are identical for all wobbling bands, as they correspond to the rotation around the 1 axis, see Eq. (11); and (iii) the interband $B(E2)$ probabilities show a linear dependence on n, as they link phonon excitations with a different number of phonons, see Eqs. (12) and (13) [16]:

$$B(E2; n, I \to n, I \pm 2) = \frac{5}{16\pi} e^2 Q_2^2, \tag{11}$$

$$B(E2; n, I \to n - 1, I - 1) = \frac{5}{16\pi} e^2 \frac{n}{I} (\sqrt{3} Q_0 x - \sqrt{2} Q_2 y)^2, \tag{12}$$

$$B(E2; n, I \to n + 1, I + 1) = \frac{5}{16\pi} e^2 \frac{n + 1}{I} (\sqrt{3} Q_0 y - \sqrt{2} Q_2 x)^2, \tag{13}$$

where Q_0 and Q_2 are the intrinsic quadrupole moments of the nuclear charge density with respect to the 1 axis, and x and y are

$$x = \sqrt{\frac{1}{2}\left(\frac{\alpha}{\hbar\omega} + 1\right)}, \quad y = \sqrt{\frac{1}{2}\left(\frac{\alpha}{\hbar\omega} - 1\right)}. \tag{14}$$

Therefore while both 3D rotation and wobbling describe excited rotational bands for which the rotational angular momentum tilts away from the 1 axis, the wobbling description demands specific quantization of the excitation energies and transition probabilities of the wobbling bands which is not required in the case of TiP bands. Nevertheless, it is possible that in some cases the two models predict bands with approximately the same nature.

The wobbling approximation is valid if the rotational angular momenta around the two axes with lower MoI is small [16]:

$$I_2^2 + I_3^2 \ll I^2, \tag{15}$$

a condition that can be rewritten as

$$f(n, I) = (2n + 1)\frac{(A_2 + A_3 - 2A_1)}{2I\sqrt{(A_2 - A_1)(A_3 - A_1)}} \ll 1. \tag{16}$$

The function $f(n, I)$ is shown in Fig. 4 for the example of Fig. 1 (rotational parameters of $A_1 = 1$, $A_2 = 4$, and $A_3 = 4$) and for the $n = 1$ and $n = 2$ wobbling bands. It is clear that the approximation condition $f(n, I) \ll 1$ is not fulfilled at low spins, where the values of $f(n, I)$ are comparable to 1. However, the function has a decreasing trend for higher I, for instance $f(n, I) < 0.15$ for ($n = 1$, $I > 20$) and ($n = 2$, $I > 34$). Therefore, wobbling phonon excitations can exist at high spins, as pointed out in [16].

One thus concludes that at low and medium spins the wobbling is a poor approximation for the TiP bands in even-even triaxial nuclei. However, at high angular momenta they start showing the characteristic features of wobbling phonon excitations, such as quantization of the excitation energies and transition probabilities. To illustrate the difference at low and medium spins the excitation energies calculated with the 3D rotating Hamiltonian and with the wobbling approximation equation are compared in Fig. 1. For a given spin I the wobbling bands show a regular energy spacing equal to the wobbling frequency $\hbar\omega$, highlighting the characteristic energy quantization of a phonon excitation; see Fig. 1(b). Contrary to that, the 3D rotation produces TiP bands with irregular relative excitation energy; see Fig. 1(a).

It is interesting to note that for the case shown in Fig. 1, one can assign a quantum number m to the TiP bands:

$$m = I - i, \tag{17}$$

which is a counterpart to the wobbling quantum number n [18]. Bands $b0$, $b1$, $b2$, etc., see Fig. 1, which are associated with projections of the rotational angular momentum on the 1 axis of I, $I-1$, $I-2$, etc., are thus assigned $m=0$, $m=1$, $m=2$, etc. Following Eq. (4) the energies of the levels of the rotational bands are

$$E(I,m) = \frac{3\hbar^2}{8\Im_0}\{I(I+4) + 3m(2I-m)\}. \tag{18}$$

This once again highlights the difference between wobbling and TiP rotation; the former requires quantization of the excitation energy with respect to the number of excited phonons n, Eq. (9), thus the energy should increase linearly with n, while the latter obeys a quadratic dependence on m, Eq. (18).

It has been suggested that the observation of wobbling bands can be used as a proof that the nuclear shape is nonaxially symmetric. In fact the observation of TiP bands (such as the sets of rotational bands shown in Fig. 1, or the rotational bands calculated for instance in Ref. [18]), seems a better evidence for triaxial nuclear shape; indeed wobbling occurs at high spins only, while TiP is present in the whole spin range.

III. TILTED PRECESSION AND WOBBLING IN ODD-MASS NUCLEI

In odd-mass triaxial nuclei the 3D rotation of the core is coupled with the angular momentum of the valence nucleon. There are two simple coupling schemes, where the angular momentum of the valence nucleon is aligned with respect to a nuclear axis; it could be aligned (i) along the axis with largest MoI, the 1 axis, or (ii) perpendicular to it. These two couplings, recently called longitudinal and transverse, respectively [1], generate rotational bands with different properties.

Assuming irrotational flow MoI the angular momentum of the core is largest along the intermediate axis. Therefore for transverse coupling the single-particle angular momentum should be orthogonal to the intermediate axis, thus aligned either along the short or along the long nuclear axes. In that case the valence nucleon should occupy an orbital at the bottom of a given subshell (particle nature and alignment along the short axis) or an orbital at the top of a given subshell (hole nature and alignment along the long axis). For longitudinal coupling the single-particle angular momentum should align along the intermediate axis, thus the valence nucleon should occupy an orbital near the middle of the shell.

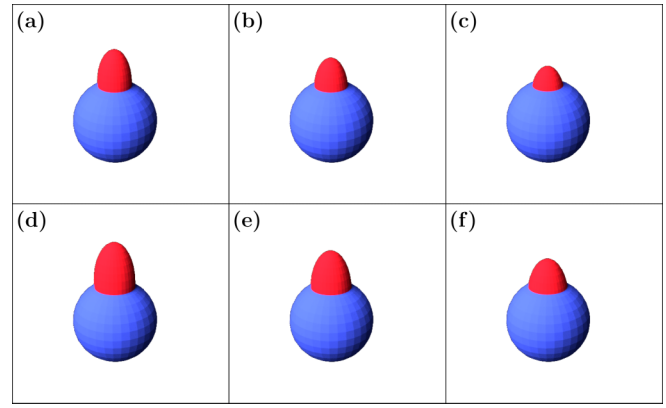

FIG. 5. As in Fig. 2, but for longitudinal coupling where the particle angular momentum j is aligned along 1 axis, thus the energy spheroid is moved by j along that axis.

The rotational Hamiltonian has a particle-hole symmetry, that is a band that corresponds to a configuration of a valence nucleon from the bottom of a subshell coupled to a core with nonaxiality of γ is identical to a band that corresponds to a nucleon from the top of the subshell coupled to a core with nonaxiality of $60^\circ - \gamma$. Therefore for $\gamma = 30^\circ$ the rotational bands for a particle configuration are identical to those for the corresponding hole configuration. In the following transverse coupling involving an odd nucleon with particle nature will be considered, as the results for the hole configuration are identical.

The rotational Hamiltonians for longitudinal and transverse coupling of the angular momenta are

$$H = A_1(I_1 - j)^2 + A_2 I_2^2 + A_3 I_3^2, \tag{19}$$

and

$$H = A_2(I_2 - j)^2 + A_1 I_1^2 + A_3 I_3^2, \tag{20}$$

respectively, as the largest MoI is along the 1 axis.

The 3D rotation in odd-mass nuclei can also be visualized using the intersection of the angular momentum sphere [see Eq. (5)] and the energy ellipsoid, which in this case is

$$E = A_1(I_1 - j)^2 + A_2 I_2^2 + A_3 I_3^2 \tag{21}$$

and

$$E = A_2(I_2 - j)^2 + A_1 I_1^2 + A_3 I_3^2 \tag{22}$$

for longitudinal and transverse coupling, respectively. Therefore the energy ellipsoid for these two couplings will be shifted by j along the 1 axis and along the 2 axis, respectively, as shown in Figs. 5 and 6. The intersection between the angular momentum sphere and the energy spheroid is a circle and represents the curve along which the total angular momentum precesses. As in even-even nuclei the 3D rotation in

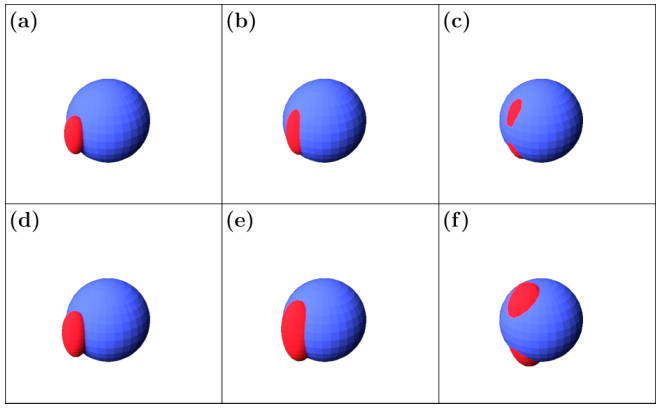

FIG. 6. As in Fig. 2, but for transverse coupling where the particle angular momentum j is aligned along 2 axis, thus the energy spheroid is moved by j along that axis.

odd-mass nuclei can be represented as a precession of the total angular momentum along the axis where the single-particle angular momentum is aligned, producing TiP bands. (Note that as shown in Figs. 5 and 6 for transverse wobbling the axis of precession changes at high spins.) Figures 7 and 8 illustrate 3D rotation for longitudinal and transverse coupling with rotational parameters of $A_1 = 1$, $A_2 = 3$, $A_3 = 6$. The intersection curve in this case is not a circle but an ellipse lying on a sphere.

To create excited rotational states for the same I one could tilt the total angular momentum away from the 1 axis (2 axis), for longitudinal (transverse) coupling, as shown in panels (d)–(f) of Figs. 5–8. For odd-mass nuclei there are two distinct ways to produce such a tilt: (i) by tilting the angular momentum of the valence nucleon, or (ii) by tilting the rotational angular momentum. In both cases the intersection of the angular momentum sphere with the energy ellipsoid corresponds to a precession of the total angular momentum around the corresponding axis with a larger tilt angle θ, producing TiP bands.

In fact, all 3D nuclear rotations can be visualized as a precession of the total angular momentum around a certain

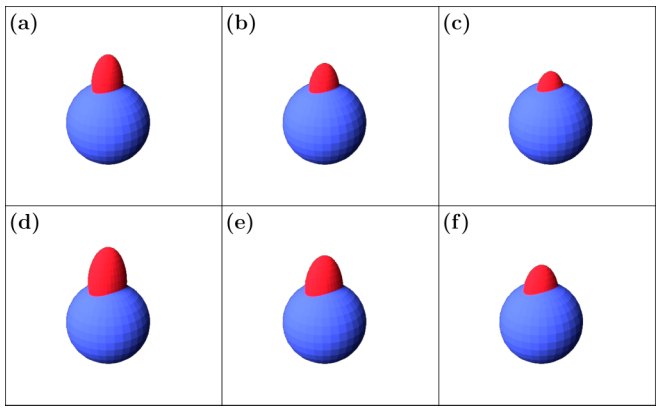

FIG. 7. As in Fig. 5, but for rotational parameters of $A_1 = 1$, $A_2 = 3$, and $A_3 = 6$.

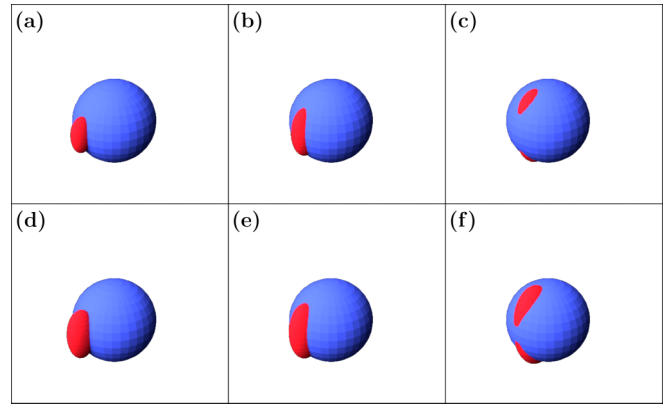

FIG. 8. As in Fig. 7, but for rotational parameters of $A_1 = 1$, $A_2 = 3$, and $A_3 = 6$.

axis, producing TiP bands. However, not all TiP bands can be approximated with wobbling. For instance the TiP bands that are produced by tilting the single-particle angular momentum away from the corresponding axis are by default incompatible with wobbling. They correspond to a change in the single-particle configuration where the odd nucleon changes into an orbital with a smaller alignment. Only the second type of TiP bands, those formed by tilting the rotational angular momentum, could in principle be compared with wobbling. Therefore to avoid excitations due to changes of the alignment of the valence nucleon its angular momentum has to be fixed to the corresponding axis [1]. The freezing of the single-particle angular momentum has been questioned. It has been pointed out that with increasing the spin the single-particle angular momentum changes orientation from perpendicular to parallel to the intermediate axis, where the angular momentum of the core is aligned [21]. It was therefore suggested that the wobbling motion is unstable for transverse wobbling and one-quasiparticle configurations. This issue was further discussed [22,23], but it is beyond the scope of the present study. In this work we intend to test whether the TiP bands for transverse coupling can be approximated with wobbling, thus in the following we adopt the description in which the angular momentum of the valence nucleon is frozen.

For transverse coupling the Hamiltonian of Eq. (20) can be rewritten as [1]

$$H \approx A_2(I - j)^2 + (A_1 - A_2')I_1^2 + (A_3 - A_2')I_3^2, \tag{23}$$

where

$$A_2' = A_2(1 - j/I), \tag{24}$$

and

$$I_2 = \sqrt{I(I+1) - I_1^2 - I_3^2} \approx \sqrt{I(I+1)}\left[1 - \frac{I_1^2 + I_3^2}{2I(I+1)}\right]. \tag{25}$$

The rotations around the 1 and 3 axes were approximated with the excitation of harmonic phonons, described with the phonon creation (c^+) and annihilation (c)

operators, [1]:

$$H \approx A_2(I-j)^2 + \tfrac{1}{2}\alpha(c^+c + cc^+) + \tfrac{1}{2}\beta(c^+c^+ + cc), \quad (26)$$

where the coefficients α and β were

$$\alpha = (A_1 + A_3 - 2A_2')I \quad \text{and} \quad \beta = (A_3 - A_1)I. \quad (27)$$

This approximation generates wobbling bands with energies of

$$E(n,I) = A_2(I-j)(I-j+1) + \hbar\omega\left(n + \tfrac{1}{2}\right), \quad (28)$$

where the wobbling frequency is

$$\hbar\omega = \sqrt{(\alpha^2 - \beta^2)} = 2I\sqrt{(A_1 - A_2')(A_3 - A_2')}. \quad (29)$$

The $B(E2)$ reduced transition probabilities for the intraband and for the interband transitions with $\Delta n = 1$ are equivalent to those for even-even nuclei [see Eqs. (11), (13), and (12)] [1], but with Q_0 and Q_2 being the intrinsic quadrupole moments of the nuclear charge density with respect to the 2 axis.

The $B(M1)$ reduced transition probabilities for interband transitions with $\Delta n = 1$ were calculated as [1]

$$B(M1, n, I \to n-1, I-1) = \frac{3}{4\pi}\frac{n}{I}[j(g_j - g_R)x]^2, \quad (30)$$

$$B(M1, n, I \to n+1, I+1) = \frac{3}{4\pi}\frac{n+1}{I}[j(g_j - g_R)y]^2, \quad (31)$$

where g_j and g_R are the g factors for the valence nucleon and the rotation, respectively.

As for even-even nuclei the wobbling motion in odd-mass nuclei shows features characteristic of its phonon nature, that is

(i) the relative excitation energy of two wobbling bands is $\Delta E = E(n,I) - E(0,I) \propto n$;
(ii) the interband transition probability $B(E2; n, I \to n-1, I-1) \propto n$;
(iii) the interband transition probability $B(M1; n, I \to n-1, I-1) \propto n$.

Note that while the quantization with respect to n is a characteristic feature of a phonon excitation, it is not necessary for TiP rotation.

It should be noted that the equations above can be applied for the case of longitudinal wobbling too, by changing the 2 and 1 axes.

For transverse wobbling the expression under the square root in Eq. (29) must be positive:

$$(A_1 - A_2')(A_3 - A_2') > 0. \quad (32)$$

For longitudinal wobbling this expression reads $(A_2 - A_1')(A_3 - A_1') > 0$ and, as in the case of even-even nuclei, is always fulfilled. For transverse wobbling, however, $A_1 < A_2$ and $A_1 < A_3$. In the cases where transverse wobbling was proposed the rotational parameters were $A_1 < A_2 < A_3$, so $A_3 - A_2'$ was positive for all I, $A_1 - A_2$ was negative, but $A_1 - A_2'$ could be positive in some spin range. The empirical evaluation of the MoI of triaxial even-even nuclei suggested that the γ dependence of the nuclear MoI is similar to that of an irrotational flow, [17]. However, for irrotational flow MoI, $\gamma = 30^\circ$, and $j = 11/2$, $A_1 - A_3'$ is positive only for states with $I = 11/2$ and $13/2$. In order to extend the spin range where wobbling might occur, the relative magnitude of the three MoI were arbitrary modified, in particular the MoI around the 2 axis was considerably increased [1–4].

As for even-even nuclei the wobbling in odd-mass nuclei was introduced as an approximation; it replaced the 3D rotation of the triaxial nucleus with a 1D rotation around a certain axis (the axis along which the single-particle angular momentum is aligned) coupled with an excitation of wobbling phonons. This approximation required that the rotations around the other two axes were small. Therefore, for longitudinal coupling the rotation around the 2 and 3 axes should be small, a condition that is equivalent to the corresponding requirement in even-even nuclei; see Fig. 4. For transverse wobbling, however, the approximation requires that the rotations around the 1 and 3 axes are small:

$$I_1^2 + I_3^2 \ll I^2. \quad (33)$$

However, as $\Im_1$ is largest, the projection of the rotational angular momentum along the 1 axis is largest and therefore this condition can hardly be satisfied. It can also be written as [1]

$$f(n,I) = (2n+1)\frac{A_1 + A_3 - 2A_2'}{2I\sqrt{(A_1 - A_2')(A_3 - A_2')}} \ll 1. \quad (34)$$

We tested this condition for several MoI parameters previously assigned to bands with proposed transverse wobbling nature; see Table I. The calculated values of the approximation condition function $f(n,I)$, for the $n = 1$ and $n = 2$ phonon bands are shown in Fig. 9.

For each set of MoI parameters the values of $f(n,I)$ were calculated for the corresponding spin range of up to $I_{\max}$. The values of the approximation condition function are large for all cases listed in Table I. For sets (i) and (ii) the values of $f(n,I)$ are larger than 0.76. As seen in Fig. 9(a) the values of $f(n,I)$ for the $n = 1$ wobbling bands are larger than 0.58 for cases (iii)–(v), and larger than 0.45 for case (vi). These large values are incompatible with the approximation condition $f(n,I) \ll 1$. As $f(n,I) \propto (2n+1)$, the values of $f(n,I)$ for the $n = 2$ wobbling bands are even higher, as shown in Fig. 9(b). They are larger than 0.75 for all cases listed in Table I. Such large values suggest that the approximation condition does not hold for the bands in ^{135}Pr and ^{105}Pd, previously interpreted as transverse wobbling [1–4].

We tested the approximation condition for the TSD bands too, see Fig. 4, using parameters of case (vii) in Table I. For the $n = 1$ wobbling band the values of the function $f(n,I)$ are larger than 0.32, and for the $n = 2$ wobbling band they are larger than 0.53, suggesting that the approximation condition is not met for these bands too. As a comparison we also plotted in Fig. 4 the approximation condition, assuming longitudinal wobbling (the valence $i_{13/2}$ proton and the dominant rotation are aligned along the short nuclear axis, and the MoI are of rigid body type; see case (viii) in Table I according to the original interpretation of these bands, for instance [21]).

TABLE I. Sets of MoI used for the suggested transverse wobbling bands. For each set the rotational parameters, together with the introduced spin dependence, are listed. In addition the angular momentum of the valence nucleon, j, and the maximal value, $I_{\max}$ [see Eq. (32)], are listed.

Set	MoI	A_1	A_2	A_3	$\Im(I)$	j	$I_{\max}$	Nucleus	Ref.
(i)	irrotational flow	1	4	4		11/2	13/2		
(ii)	modified	1	3	6		11/2	15/2		[1]
(iii)	modified	1	1.6	4		11/2	29/2		[1]
(iv)	fitted to ^{135}Pr	0.024	0.039	0.125		11/2	27/2	^{135}Pr	[1]
(v)	fitted to ^{135}Pr	0.068	0.093	0.278	$\propto 1 + cI$	11/2	45/2	^{135}Pr	[2,3]
(vi)	fitted to ^{105}Pd	0.085	0.134	0.394	$\propto\sqrt{1 + bI(I+1)}$	11/2	29/2	^{105}Pd	[4]
(vii)	fitted to ^{163}Lu	0.0078	0.0089	0.0385		13/2	85/2	^{163}Lu	[1]
(viii)	rigid MoI	0.033	0.030	0.036		13/2		^{163}Lu	[21]

In this case the values of $f(n, I)$ are similar to those for even-even nuclei and show a steady decrease; they are smaller than 0.15 (i) for $n = 1$ and $I > 19.5$, and (ii) for $n = 2$ and $I > 33.5$. Note that contrary to the one-quasiparticle bands in ^{135}Pr and ^{105}Pd, the TSD bands are observed up to very high spins, e.g., up to $I = 97/2$ in ^{163}Lu [6], where the approximation condition (assuming the original interpretation as longitudinal wobbling) is satisfied.

Contrary to the case of longitudinal wobbling, the approximation condition for transverse wobbling is not satisfied for the cases in Table I because it demands the rotation around the axis with largest MoI to be small. We examined the function $f(n, I)$ trying to evaluate its lowest possible values for $j = 11/2$. It is noticeable that assuming a larger MoI along the 2 axis increases the spin range of the wobbling band, $I_{\max}$, and somewhat decreases the values of $f(n, I)$ at medium spins; compare for instance cases (i) and (iii) in Fig. 9(a). We thus calculated $f(n, I)$ with the maximum value of $\Im_2$, that is $\Im_2 = \Im_1$; see the dashed red line in Fig. 9(a). (Note that in this case the nucleus has axially symmetric shape, which means that the bands cannot be associated with wobbling.) However, even in this case the values of $f(n, I)$ are high at low spins, reaching a value of $f(n, I) = 0.34$ at spin of $I = 29/2$ for the $n = 1$ band. The absolute minimum of the $f(n, I)$ function is obtained when all three MoI are equal, $\Im_1 = \Im_2 = \Im_3$; see the solid black line in Fig. 9(a) with values between 0.55 and 0.21 in the spin range of (11/2, 29/2). It is obvious that even in that case, where the nucleus is spherical, the values of $f(n, I)$ are still large.

The lowest possible values of the approximation condition function $f(n, I)$ for $n = 2$ correspond to dashed-dotted red and the dashed black lines in Fig. 9(b) calculated with the assumptions of $\Im_2 = \Im_1$ and $\Im_1 = \Im_2 = \Im_3$, respectively. For the spin range of (11/2, 29/2) the function $f(n, I)$ has values larger than 0.57 for the former case, and larger then 0.34 for the latter case. It is therefore evident that the approximation

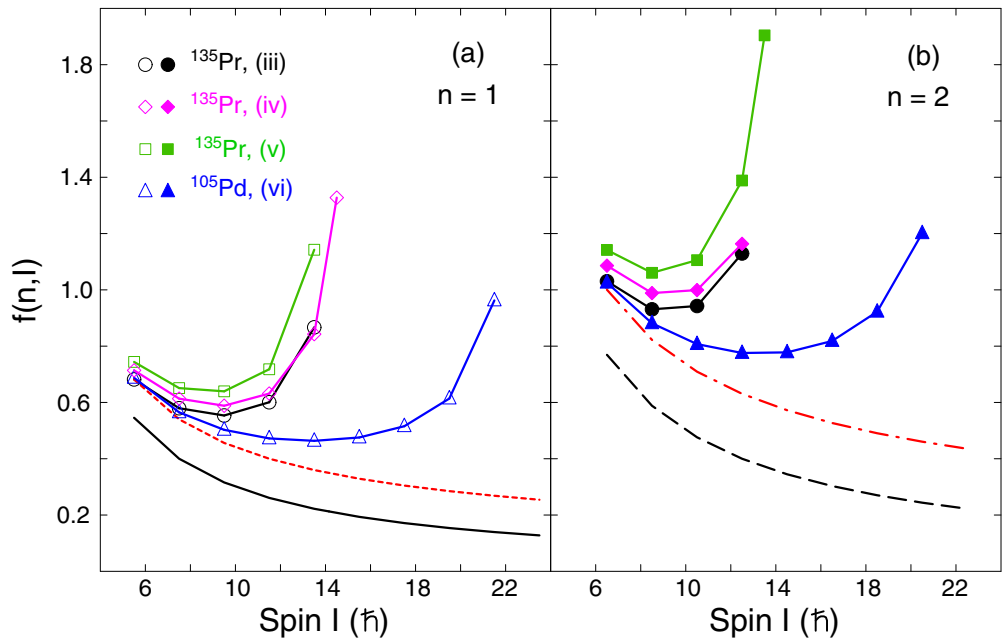

FIG. 9. Approximation condition function $f(n, I)$ for $j = 11/2$, various sets of MoI listed in Table I and for (a) $n = 1$ and (b) $n = 2$ phonon excitations. The dotted and dashed-dotted red lines correspond to $\Im_2 = \Im_1$ and the solid and dashed black lines to $\Im_1 = \Im_2 = \Im 3$.

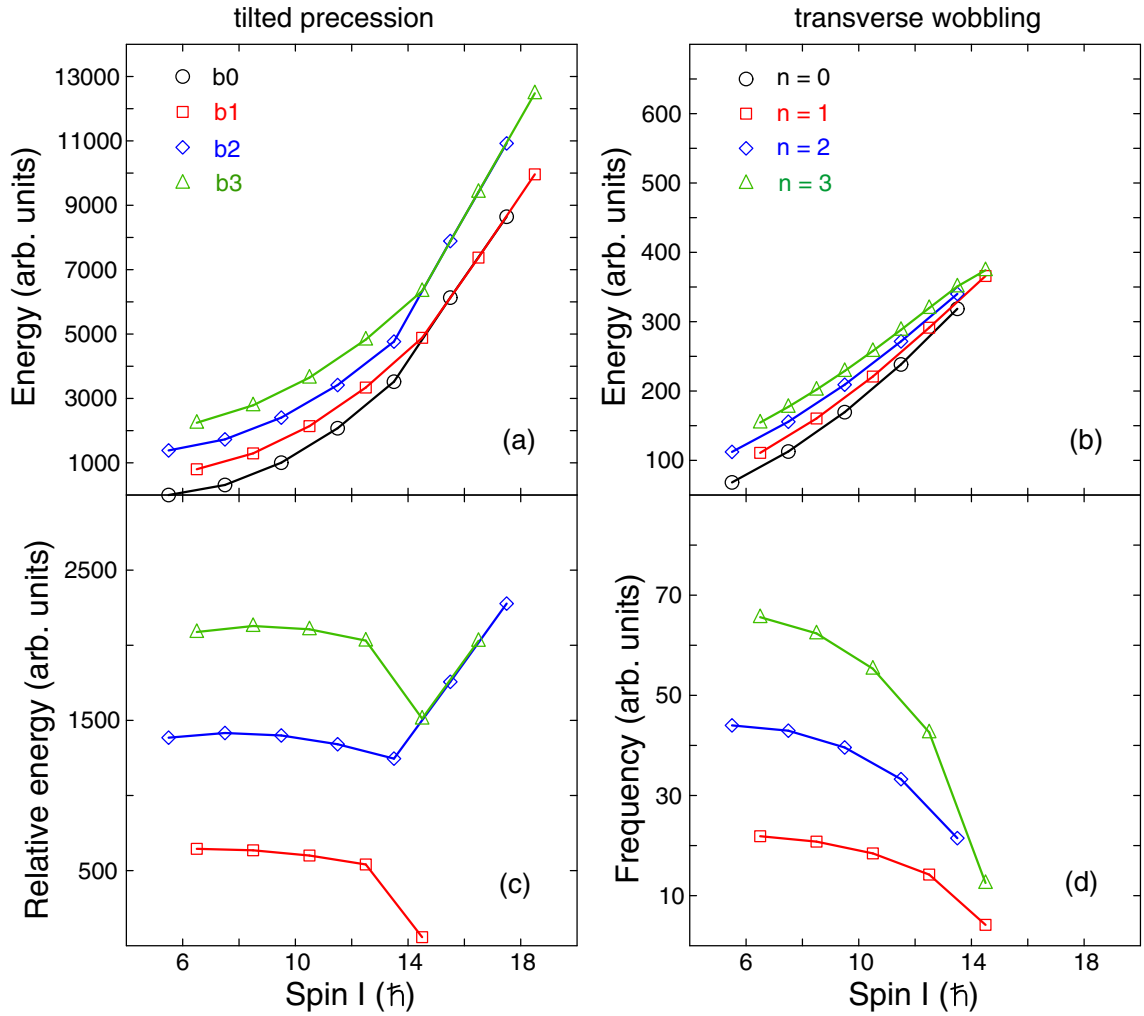

FIG. 10. Excitation energy vs spin for rotational bands with $j = 11/2$, transverse coupling of the angular momenta, and (a) tilted precession rotation and (b) wobbling phonon approximation. Panels (c) and (d) illustrate the relative excitation energy of the bands with respect to the yrast band for the TiP and wobbling bands, respectively. The calculations assume the same rotational parameters, case (iii) of Table I.

condition $f(n, I) \ll 1$ cannot be fulfilled for typical $j = 11/2$ bands, reasonable MoI values, and within the spin range where these bands are observed.

Therefore for transverse coupling of the angular momenta the wobbling approximation is a bad approximation for the 3D rotating Hamiltonian. This suggests that the transverse wobbling approximation is obtained with simplifying assumptions that ignore something that is not negligible. It indicates that the wobbling motion and the TiP rotation are not similar, that they should be considered as bands with fundamentally different nature.

To illustrate the difference between the TiP rotation and the transverse wobbling approximations, the corresponding bands are compared for $j = 11/2$ and with the same MoI parameters [of case (iii), see Table I]. The excitation energies of the bands produced by the two models are shown in Figs. 10(a) and 10(b). The wobbling approximation generates distinct phonon-type features of the bands, such as the same relative excitation energy between bands with $\Delta n = 1$; see Fig. 10(b). For transverse wobbling the relative excitation energy of the bands (the wobbling frequency) decreases smoothly for all bands until near $I_{\max}$ where all wobbling bands become degenerate in energy, as shown in Figs. 10(b) and 10(d). Above $I_{\max}$ the wobbling ceases. Contrary to that, the TiP bands (calculated with the QTR model [24]) are grouped in pairs of $E2$ sequences with opposite signature; see Fig. 10(a). The partner bands in each pair show a considerable energy difference at low spins, which remains almost unchanged, until the two partner bands become degenerate. Note that the bands in each pair become degenerate, but the different pairs remain well separated in energy. The relative excitation energy of the TiP bands with respect to $b0$, shown in Fig. 10(c), reflects again the fact that the bands couple in pairs.

Considerable differences between the TiP and the wobbling bands are also observed in the trends of the reduced interband $B(E2)$ and $B(M1)$ transition probabilities, as shown in Fig. 11. For instance the wobbling bands show interband reduced transition probabilities $B(n, I \to n-1, I-1)$ that are proportional to the number of excited phonons n; see Figs. 11(b) and 11(d). For instance, the ratio of $B(M1; n =$

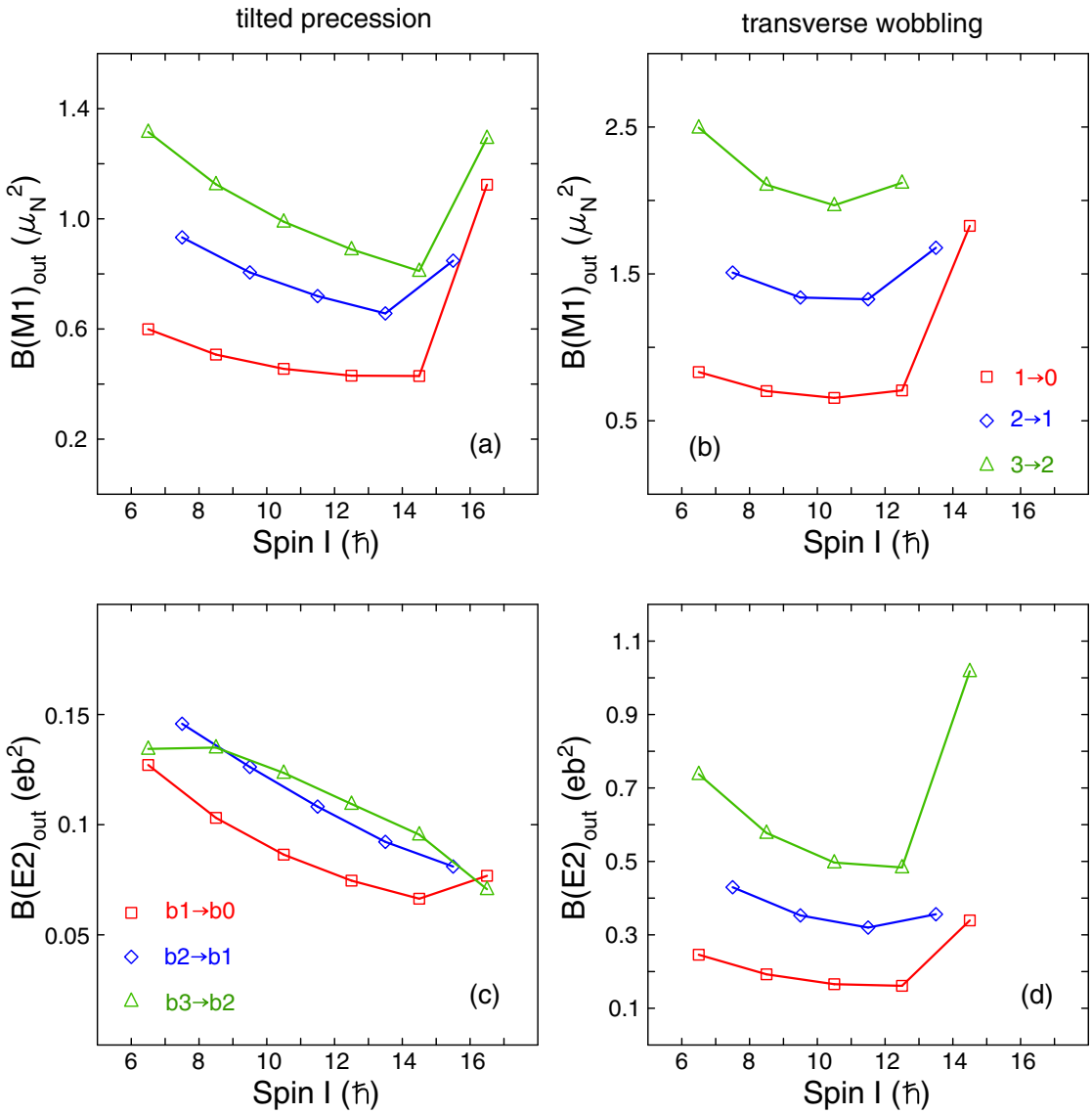

FIG. 11. Transition probabilities calculated with QTR for TiP bands and with the wobbling equations for transverse wobbling bands and with the same rotational parameters as in Fig. 10 and the same quadrupole moments.

$2, I \to n = 1, I-1)/B(M1; n = 1, I \to n = 0, I-1) = 2$ and $B(M1; n = 3, I \to n = 2, I-1)/B(M1; n = 1, I \to n = 0, I-1) = 3$. Similarly, $B(E2; n = 2, I \to n = 1, I-1)/B(E2; n = 1, I \to n = 0, I-1) = 2$ and $B(E2; n = 3, I \to n = 2, I-1)/B(E2; n = 1, I \to n = 0, I-1) = 3$. Contrary to that, these ratios are not integer numbers for the TiP bands, as seen in Figs. 11(a) and 11(c). The difference in the transition probability ratios for the two types of bands is due to their different nature—phonon excitations for the wobbling bands and tilted precession for the TiP bands.

It is known that the interband $\Delta I = 1$ transitions that link wobbling bands with $\Delta n = 1$ have a large unstretched $E2$ contribution. A large mixing ratio exhibited by such transitions has been considered as an observation supporting the wobbling nature of the bands. However, large mixing ratios are a characteristic feature of other types of bands too, for instance, the decays of the $K = 2$ γ bands towards the ground-state band in even-even axially symmetric nuclei proceeds mainly through an unstretched $E2$ component. Furthermore large mixing ratios are also a characteristic feature for the TiP bands. In fact the calculated $B(E2)$ transition probabilities for the unstretched $E2$ component of the $b1 \to b0$, $b2 \to b1$, $b3 \to b2$ linking transitions are large and similar to those of the intraband transitions ($b0 \to b0$, $b1 \to b1$, etc.).

Therefore there is, in general, a distinct difference in the nature of the TiP bands (tilted procession bands, calculated with QTR model) and the wobbling bands (phonon excitations, calculated with the wobbling approximation equations). However (i) at high spins and for even-even nuclei with zero-quasiparticle configurations, and (ii) at high spins and for one-quasiparticle bands with longitudinal coupling of the angular momenta, the TiP becomes approximately similar to the wobbling phonon description, as in that case the wobbling approximation condition is satisfied. Contrary to that for typical one-quasiparticle configurations

with transverse coupling of the angular momenta the approximation is not valid, suggesting different underlying physics.

IV. SUMMARY

All rotations in a triaxial nucleus can be represented as a precession of the total angular momentum around a certain axis. The excited bands represent a tilted precession of the angular momentum away from that axis. In this work the bands produced by such a rotation are called tilted precession (TiP) bands. Their features are predicted by the QTR model. Only in some cases, for instance, at high spins and for zero-quasiparticle bands in even-even nuclei or for one-quasiparticle bands with longitudinal coupling of the angular momenta, the TiP bands can be approximated with a coupling of rotation and excitation of wobbling phonons. For transverse coupling of the angular momenta and for one-quasiparticle configurations the TiP and the wobbling bands have distinctly different nature. Therefore it is not justified to use the QTR model as a theoretical description of transverse wobbling bands as this model produces TiP bands and not wobbling. This suggests that the bands observed previously in ^{135}Pr and ^{105}Pd that were at the time interpreted as transverse wobbling based on a comparison with the QTR model, are in fact TiP bands. The transverse wobbling bands, contrary to TiP bands, should exhibit the quantization (that is characteristic for all phonon excitations) of their excitation energies and transition probabilities. It has been discussed that the observation of wobbling bands is an evidence for the presence of a stable triaxial deformation, but the presence of TiP bands seems an easier criterion, because the wobbling (when possible) forms at high spins only, while TiP bands can appear for both low and high spins.

ACKNOWLEDGMENTS

This work was based on research supported in part by the National Research Foundation of South Africa (Grants No. 116666, No. 109134, No. 103478, and No. 91446), and by the French Ministry of Foreign Affairs and the Ministry of Higher Education and Research, France (PHC PROTEA Grant No. 42417SE).

[1] S. Frauendorf and F. Dönau, Phys. Rev. C **89**, 014322 (2014).
[2] J. T. Matta, U. Garg, W. Li, S. Frauendorf, A. D. Ayangeakaa, D. Patel, K. W. Schlax, R. Palit, S. Saha, J. Sethi, T. Trivedi, S. S. Ghugre, R. Raut, A. K. Sinha, R. V. F. Janssens, S. Zhu, M. P. Carpenter, T. Lauritsen, D. Seweryniak, C. J. Chiara *et al.*, Phys. Rev. Lett. **114**, 082501 (2015).
[3] N. Sensharma, U. Garg, S. Zhu, A. D. Ayangeakaa, S. Frauendorf, W. Li, G. H. Bhat, J. A. Sheikh, M. P. Carpenter, Q. B. Chen, J. L. Cozzi, S. S. Ghugre, Y. K. Gupta, D. J. Hartley, K. B. Howard, R. V. F. Janssens, F. G. Kondev, T. C. McMaken, R. Palit, J. Sethi *et al.*, Phys. Lett. B **792**, 170 (2019).
[4] J. Timár, Q. B. Chen, B. Kruzsicz, D. Sohler, I. Kuti, S. Q. Zhang, J. Meng, P. Joshi, R. Wadsworth, K. Starosta, A. Algora, P. Bednarczyk, D. Curien, Zs. Dombrádi, G. Duchêne, A. Gizon, J. Gizon, D. G. Jenkins, T. Koike, A. Krasznahorkay *et al.*, Phys. Rev. Lett. **122**, 062501 (2019).
[5] S. W. Ødegård, G. B. Hagemann, D. R. Jensen, M. Bergström, B. Herskind, G. Sletten, S. Törmänen, J. N. Wilson, P. O. Tjøm, I. Hamamoto, K. Spohr, H. Hübel, A. Görgen, G. Schönwasser, A. Bracco, S. Leoni, A. Maj, C. M. Petrache, P. Bednarczyk, and D. Curien, Phys. Rev. Lett. **86**, 5866 (2001).
[6] D. R. Jensen, D. R. Jensen, G. B. Hagemann, I. Hamamoto, S. W. Ødegård, M. Bergström, B. Herskind, G. Sletten, S. Törmänen, J. N. Wilson, P. O. Tjøm, K. Spohr, H. Hübel, A. Görgen, G. Schönwasser, A. Bracco, S. Leoni, A. Maj, C. M. Petrache, and P. Bednarczyk, and D. Curien, Nucl. Phys. A **703**, 3 (2002).
[7] G. Schönwaßer, H. Hübel, G. B. Hagemann, P. Bednarczykc, G. Benzoni, A. Bracco, P. Bringel, R. Chapman, D. Curien, J. Domscheit, B. Herskind, D. R. Jensen, S. Leoni, G. Lo Bianco, W. C. Ma, A. Maj, A. Neußer, S. W. Ødegård, C. M. Petrache, D. Roßbach *et al.*, Phys. Lett. B **552**, 9 (2003).
[8] P. Bringel, G. B. Hagemann, H. Hübel, A. Al-khatib, P. Bednarczyk, A. Bürger, D. Curien, G. Gangopadhyay, B. Herskind, D. R. Jensen, D. T. Joss, Th. Kröll, G. Lo Bianco, S. Lunardi, W. C. Ma, N. Nenoff, A. Neußer-Neffgen, C. M. Petrache, G. Schönwasser, J. Simpson *et al.*, Eur. Phys. J. A **24**, 167 (2005).
[9] H. Amro, W. C. Ma, G. B. Hagemann, R. M. Diamond, J. Domscheit, P. Fallon, A. Görgen, B. Herskind, H. Hübel, D. R. Jensen, Y. Li, A. O. Macchiavelli, D. Roux, G. Sletten, J. Thompson, D. Ward, I. Wiedenhöver, J. N. Wilson, and J. A. Winger, Phys. Lett. B **553**, 197 (2003).
[10] G. Hagemann, Eur. Phys. J. A **20**, 183 (2004).
[11] D. J. Hartley, R. V. F. Janssens, L. L. Riedinger, M. A. Riley, A. Aguilar, M. P. Carpenter, C. J. Chiara, P. Chowdhury, I. G. Darby, U. Garg, Q. A. Ijaz, F. G. Kondev, S. Lakshmi, T. Lauritsen, A. Ludington, W. C. Ma, E. A. McCutchan, S. Mukhopadhyay, R. Pifer, E. P. Seyfried *et al.*, Phys. Rev. C **80**, 041304(R) (2009).
[12] D. J. Hartley, R. V. F. Janssens, L. L. Riedinger, M. A. Riley, X. Wang, A. Aguilar, M. P. Carpenter, C. J. Chiara, P. Chowdhury, I. G. Darby, U. Garg, Q. A. Ijaz, F. G. Kondev, S. Lakshmi, T. Lauritsen, A. Ludington, W. C. Ma, E. A. McCutchan, S. Mukhopadhyay, R. Pifer *et al.*, Phys. Rev. C **83**, 064307(R) (2011).
[13] I. Hamamoto, Phys. Rev. C **65**, 044305 (2002).
[14] I. Hamamoto and G. B. Hagemann, Phys. Rev. C **67**, 014319 (2003).
[15] K. Tanabe and K. Sugawara-Tanabe, Phys. Rev. C **73**, 034305 (2006).
[16] A. Bohr and B. Mottelson, *Nuclear Structure Volume II* (W. A. Benjamin, New York, 1975).
[17] J. M. Allmond and J. L. Wood, Phys. Lett. B **767**, 226 (2017).
[18] J. Meyer-ter-Vehn, Nucl. Phys. A **249**, 111 (1975).
[19] F. Q. Chen, J. Meng, and S. Q. Zhang, Phys. Lett. B **785**, 211 (2018).

[20] F. Q. Chen, Q. B. Chen, Y. A. Luo, J. Meng, and S. Q. Zhang, Phys. Rev. C **96**, 051303(R) (2017).
[21] K. Tanabe and K. Sugawara-Tanabe, Phys. Rev. C **95**, 064315 (2017).
[22] S. Frauendorf, Phys. Rev. C **97**, 069801 (2018).
[23] K. Tanabe and K. Sugawara-Tanabe, Phys. Rev. C **97**, 069802 (2018).
[24] P. B. Semmes and I. Ragnarsson, in *Proceedings of the International Conference on High-Spin Physics and Gamma-Soft Nuclei, Pittsburg, 1990*, edited by J. X. Saladin, R. A. Sorenson, and C. M. Vincent (World Scientific, Singapore, 1991), p. 500; in *Future Directions in Nuclear Physics with* 4π *Gamma Detection Systems of the New Generation*, AIP Conf. Proc. 259, edited by J. Dudek and B. Haas (AIP, Woodbury, NY, 1992), p. 566.